Implosion of an Aluminum Plasma Jet onto a Coaxial Wire: A Z Pinch with Enhanced Stability and Energy Transfer

F. J. Wessel[a] and B. Etlicher

Laboratoire de Physique des Milieux Ionises, Laboratoire du Centre National de la Recherche Scientifique, Ecole Polytechnique, 91128 Palaiseau, France

P. Choi

The Blackett Laboratory, Imperial College of Science, Technology and Medicine, London SW7 2BZ, United Kingdom

(Received 25 March 1992)

We describe Z-pinch experiments imploding an aluminum-plasma jet onto a coaxial, micron-diameter wire. Spatially resolved x-ray pinhole images and time resolved x-ray data indicate that energy is supplied initially to the aluminum-jet plasma and subsequently transferred to the wire. The resultant pinch appears more uniform (stable) than a wire-only or jet-only pinch and demonstrates that an imploding-plasma liner will couple energy from a pulsed-power generator to a micron-diameter-sized plasma channel.

PACS numbers: 52.55.Ez, 52.80.Qj

High-density pinches, obtained by passing a high-power discharge through a conducting or nonconducting micron-diameter fiber, are actively studied as a source of energetic x-ray radiation and means to achieve thermonuclear fusion. 2D computer simulations [1] and experiments [2,3] of fiber pinches concur that a surface-ablation plasma is initially liberated from the fiber, subsequently undergoes rapid expansion to large radius during current rise, and finally recompresses. During recompression instabilities occur [4–7] which inhibit assembly to a uniform high density-temperature plasma. The presence of an (incompletely ionized) cold core mediates gross disruption but does not inhibit instability growth [8].

Axial uniformity is an important prerequisite for radiative collapse [9–11] that requires a sustained Bennett-like equilibrium during energy delivery and heating of the discharge plasma with a current rate of rise of order [12] $dI/dt \sim 10^{15}$ A s^{-1}, assuming an initial plasma temperature of $T_e < 1$ eV. Using a pulsed-power system to drive a 10-μm-diam fiber would require a driver voltage of $V = LdI/dt = 25$ MV (assuming an inductance of $L \sim 25$ nH), which is beyond present technology.

Alternatively, the rising-current pulse may be supported in a preformed, large-diameter liner or solid-column plasma which implodes onto a coaxial, small-diameter target. Proper electrical-hydrodynamic timing may provide a staged-energy transfer [13] and large values of dI/dt. Previous studies, involving annular hollow-shell implosions onto various targets [14], have shown such staged implosions to be quite stable [15]. In the present study a coaxial wire or fiber is embedded in an aluminum-jet-plasma Z pinch, i.e., pinch on wire (POW). The jet serves as a source of uniform preionization to carry the rising-current pulse and to tamper coronal expansion from the target during jet implosion.

These POW experiments were evaluated on GAEL, a 2- Ω, 0.1-TW, 225-kA, 110-ns pulse-line generator [16]. The load plasma was prepared from an exploded 5-μm-thick Al foil, collimated into a 3-mm-diam column between discharge electrodes (A–K gap of 9 mm), and imploded onto wires of Cu and W. The jet mass per unit length was approximately 15–30 μg/cm, adjusted by varying the delay between the foil explosion and the main-current pulse [17], with a wire mass in the range 15–20 μg/cm (diameter dependent). Figure 1(a) illustrates the experimental arrangement. Diagnostics include

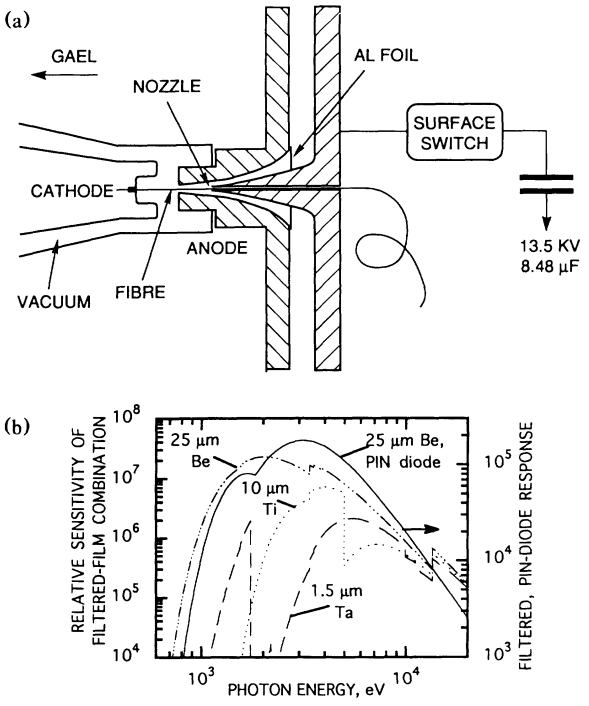

FIG. 1. Schematic illustration of (a) the pinch-load region showing the anode-cathode electrodes, the aluminum-jet nozzle, coaxial wire, and (b) calculated sensitivity of the x-ray filtered SB-392 film used in the pinhole camera and filtered p-i-n diode detectors [18].

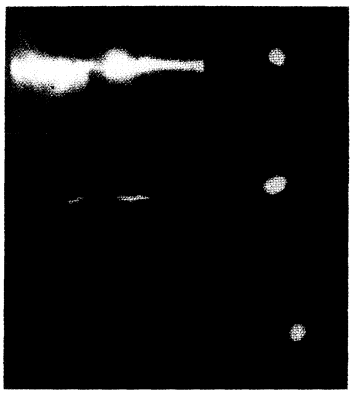

FIG. 2. Time-integrated x-ray pinhole images of an Al jet-only discharge: shot No. 1350, foil delay $\simeq 12.6$ μs. Pinhole diameter/filter thickness: panel (A), 50-μm pinhole/25-μm Be; panel (B), 50-μm pinhole/1.5-μm Ta; panel (C), 200-μm pinhole/10-μm Ti filter.

load-current monitor, x-ray-filtered p-i-n diode detector, and a time-integrated multipinhole-multifilter x-ray camera. An x-ray filtered streak camera was also used, although absolute-timing problems precluded our reporting these unreliable data. Figure 1(b) displays the calculated response [18] of the x-ray filtered SB-392 film used in the x-ray pinhole camera and filtered p-i-n diode detector.

Detailed descriptions of the aluminum-jet characteristics, jet-only implosions, and time-dependent current, x-ray pulse, streak information are provided elsewhere [19]. These measurements indicate that a high-density, sub-mm-diam pinch is formed which remains stable for 20–40 ns. The x-ray pinhole photographs shown in Fig. 2 characterize a typical Al jet-only discharge (shot No. 1350, foil delay, i.e., time between foil explosion and the energization of the accelerator, $\simeq 12.6$ μs) under conditions where the mass/unit length (M/L) is optimized for maximum x-ray emission and pinhole image uniformity. Decreasing M/L, by adjusting the foil decay to 7 μs, slightly decreases the x-ray intensity and final-pinch diameter, due to lower density, but not the overall appearance of the plasma column. In Fig. 2 two axial regions of hot-spot radiation are observed (note that the bright spot on the right-hand side of each image is an artifact introduced by labeling the images, after film development). Low-energy filtration (panel A: 50-μm pinhole, 25-μm Be filter, cutoff energy ~ 1 keV) shows a well-defined emission contour, below the Al K edge, ~ 1.6 keV, with a diameter of $\simeq 400$ μm and less near the pinch center. Medium-energy filtration (panel B: 50-μm pinhole, 1.5-μm Ta filter, cutoff energy ~ 1.4 keV) more precisely localizes the emission contour near the aluminum K edge in an extended axial region; the reduced sensitivity of this channel above 3 keV does not contribute to this image. High-energy filtration (panel C: 200-μm pinhole, 10-μm Ti filter, cutoff energy ~ 2 keV) indicates little energy contribution above 2 keV and further localizes the hot-spot radiation.

Figures 3(a) and 3(b) display pinhole images for shots No. 1379 and No. 1384, 10-μm W and 20-μm Cu wire-only discharges, respectively. These emission contours are typical of exploding-wire pinches, i.e., dominated by hot-spot radiation distributed along the length of the pinch. The Cu wire radiation is more radially distended, intense, and correlated with fewer hot spots than the W wire images, for all energy filtrations (panels A–C). Compared to the jet-only pinch (cf. Fig. 2) the emission contours in Fig. 3 were characterized by larger diameter, hence greater x-ray energy and intensity (consistent with the observed larger amplitude peak-load current and p-i-n diode wave forms), and less axial uniformity (i.e.,

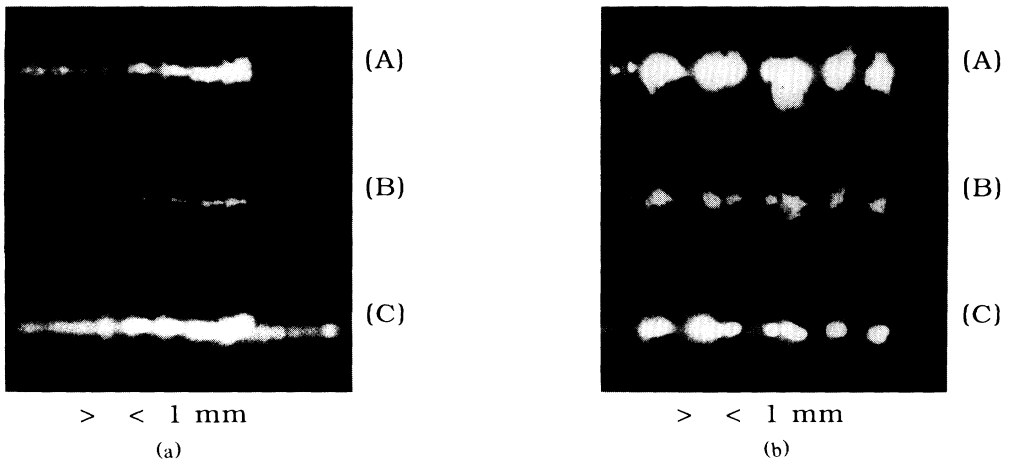

FIG. 3. X-ray pinhole images for two wire-only discharges: (a) shot No. 1379, 10-μm-diam W wire; (b) shot No. 1384, 20-μm-diam Cu wire. Same pinhole/filter combinations as Fig. 2.

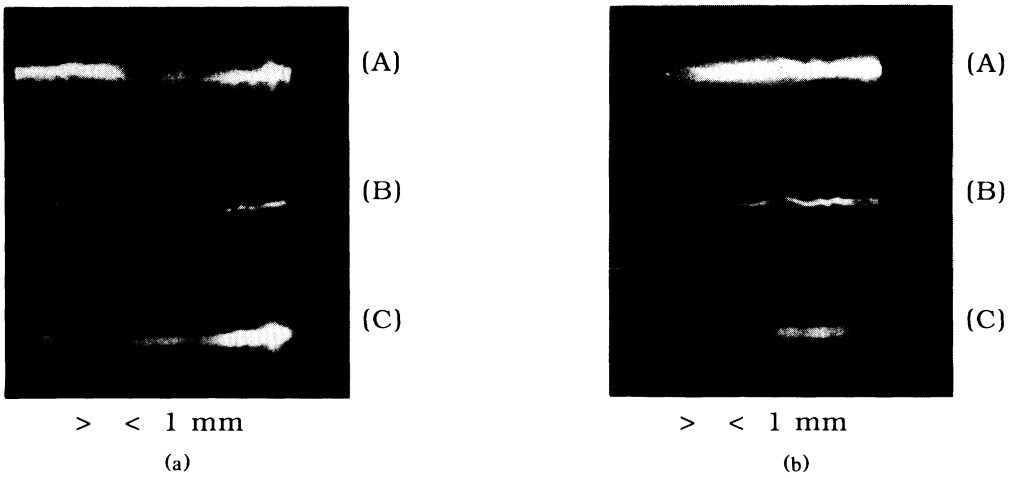

FIG. 4. X-ray pinhole images for two POW discharges: (a) shot No. 1378, 10-μm-diam W wire, foil delay 14.3 μs, and (b) shot No. 1386, 20-μm-diam Cu, foil delay 14.8 μs. Same pinhole/filter combinations as Fig. 2.

more hot spots).

Figures 4(a) and 4(b) display x-ray images for two pinch-on-wire discharges (shot No. 1378, 10-μm-diam W wire, foil delay 14.3 μs, and shot No. 1386, 20-μm diam Cu wire, foil delay 14.8 μs); note the obvious differences in uniformity compared to the wire-only discharges of Fig. 3. The relative energy distribution among the three x-ray filtered channels is similar to the preceding figure, being noticeably shifted to higher energy compared to the jet-only pinch. The POW discharges were also significantly more uniform than the jet-only or wire-only pinches for all fiber materials tested, including 30-μm SiO_2 and 25-μm Al (the results of which are not shown here). The low-energy filtered images (Fig. 4, panel A) have the largest emission diameter, approximately 600 μm diameter, associated with aluminum K-shell radiation. Nevertheless, a significant amount of energy is still observed at higher energy (panels B and C). Comparing panels A and C, we note that the high-energy radiation, $E > 2$ keV, is concentrated within a 200- to 300-μm-diam column; in Fig. 4(a) we note that the main discharge is offset to one side with a discontinuous intensity near the pinch center while the wire remains well coupled, radiating at higher energy in Fig. 4(a), panel C.

Decreasing the liner mass to unit length ratio in the POW configuration improves coupling to the fiber, as shown in Fig. 5 (shot No. 1341, 10-μm-diam W wire, foil delay 7.6 μs) which reveals a uniform hot plasma surrounding the wire; in this figure the wire is clearly delineated by its curvature, resulting from poor mounting prior to the shot. The low intensities of the low-energy images at large radius (panels A and B) indicate that the outer plasma remains cold; some low-energy Al plasma radiation is still visible at large diameter in panel B (note this is the lowest-cutoff-energy channel). The large-diameter, intense-emission contour observed at high energy in panel C indicates a core temperature above 2 keV. Compared to panels A and B the larger diameter is consistent with pneumbral blurring from the large-diameter pinhole (pinch-to-pinhole distance of 7.7 cm, and pinch-to-film distance of 13.7 cm). Also, the spectrum in Fig. 5 is noticeably shifted to higher energy and is axially more uniform than the POW discharges of Fig. 4. Improved coupling, for smaller foil delay, is reasonable since lower total mass probably results in a higher energy ion. Plasma preheat during implosion may also be a factor.

Figure 6 displays time-resolved load-current and p-i-n diode signals (25-μm-thick Be filter, bare BPX 65 p-i-n diode) for shot No. 1378 which were typical of most POW shots; the sudden jump in current observed approx-

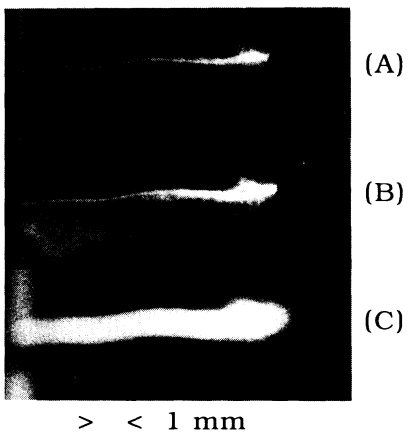

FIG. 5. X-ray pinhole images of a POW discharge with reduced liner mass: shot No. 1341, 10-μm-diam W, foil delay 7.6 μs. Pinhole diameter/filter thickness: panel (A), 50-μm pinhole/25-μm Be filter; panel (B), 50-μm pinhole/10-μm Be filter; panel (C), 400-μm pinhole/10-μm Ti filter.

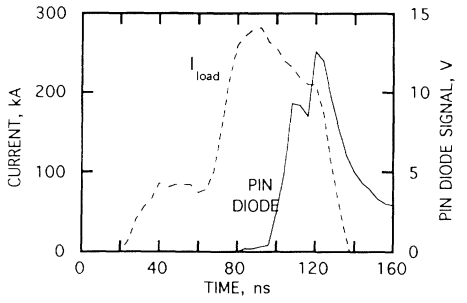

FIG. 6. Time-resolved load current and filtered p-i-n diode signal (2-μm-thick Be filter over a bare BPX 65 p-i-n diode) for a POW discharge: shot No. 1378, 10-μm-diam W wire, foil delay 12.6 μs.

imately 70 ns into the discharge is associated with the transition from the prepulse current to the full current that is characteristic of capacitive coupling between the water line and load section in generators of the present design. At maximum compression the POW pinch current was routinely $(0.5-2)\times$ lower than in jet-only or wire-only discharges and the (10–90)% radiation-pulse rise time was sharper (typically 3–10 ns for the POW shots versus 5–15 ns for fiber-only and jet-only discharges); such observations are consistent with recent reports from the Soviet Union [13]. This suggests that on-axis assembly and energy conversion in the POW is more rapid than its non-POW counterparts, possibly due to the high final impedance resulting from an axially uniform, small-diameter pinch. Although calibrated measurements of the total radiated energy were not made, larger amplitude signals observed on an array of three differentially filtered p-i-n diodes did confirm that the radiated energies were approximately $(0.5-2)\times$ greater in the wire-only versus POW discharges and POW versus puff-only shots, even though the pinch current was smallest in the POW shots. Among these detectors the relative variations in signal amplitude were also consistent with the apparent wavelength shift to higher energy recorded in the x-ray pinhole images.

In summary, we have tested a discharge-load configuration consisting of a wire embedded in a current-carrying aluminum-jet plasma. This configuration results in a column of high-temperature plasma which does not manifest typical large-scale inhomogeneities characteristic of exploding-wire or aluminum-plasma-jet pinches. These experiments demonstrate that low-impedance, high-power generators will couple to thin-wire loads in the presence of a uniformly prepared, coaxially preinjected jet, providing axially uniform final pinches, decreased radiation rise time, and shift to higher spectral energy compared to conventional exploding-wire pinches or aluminum-jet pinches.

Special thanks are given to Sophie Attelan and Claude Rouille for their experimental assistance, Jean Claude Gauthier for his assistance in image interpretation, and Rick Spielman for generously supplying the x-ray detector code. This work was supported by ETCA/CEG under Contract No. 420/115/01.

[a]Present address: University of California, Department of Physics, Irvine, CA 92717-4575.

[1] I. R. Lindemuth, G. H. McCall, and R. A. Nebel, Phys. Rev. Lett. **62**, 264 (1989).

[2] J. D. Sethian, A. E. Robson, K. A. Gerber, and A. W. DeSilva, Phys. Rev. Lett. **59**, 892 (1987).

[3] J. E. Hammel and D. W. Scudder, in *Proceedings of the Fourteenth European Conference on Controlled Fusion and Plasma Physics,* edited by F. Engelmann and J. L. Alvarez Rivas (European Physical Society, Petit-Lancy, Switzerland, 1987), Pt. 2, p. 450.

[4] C. Stalling, K. Nielsen, and R. Schneider, Appl. Phys. Lett. **29**, 404 (1976).

[5] S. M. Zakharov, G. V. Ivanankov, A. A. Kolomenskii, S. A. Pikuz, and A. I. Samokhin, Fiz. Plazmy **9**, 469 (1983) [Sov. J. Plasma Phys. **9**, 271 (1983)].

[6] L. E. Aranchuk, S. L. Bogolyubskii, G. S. Volkov, V. D. Korolev, Yu. V. Koba, V. I. Liksonov, A. A. Lukin, L. B. Nikandrov, O. V. Telkovskaya, M. V. Tulupov, A. S. Chernenko, V. Ya. Tsarfin, and V. V. Yankov, Fiz. Plazmy **12**, 1324 (1986) [Sov. J. Plasma Phys. **12**, 765 (1986)].

[7] E. S. Figura, G. H. McCall, and A. E. Dangor, Phys. Fluids B **3**, 2835 (1991).

[8] I. R. Lindemuth, Phys. Rev. Lett. **65**, 179 (1990).

[9] S. I. Braginskii, *Plasma Physics and Controlled Fusion* (Pergamon, New York, 1961), p. 135.

[10] R. S. Pease, Proc. Phys. Soc. London B **70**, 445 (1957).

[11] S. I. Braginskii and V. D. Shrafranov, in *Plasma Physics and the Problem of Controlled Thermonuclear Reactions,* edited by M. A. Leontovich (Pergamon, New York, 1959), Vol. II, pp. 39–126.

[12] J. W. Shearer, Phys. Fluids **19**, 1426 (1976).

[13] V. P. Smirnov, Plasma Phys. Controlled Fusion **33**, 1697 (1991).

[14] R. B. Spielman, M. K. Matzen, M. A. Palmer, P. B. Rand, T. W. Hussey, and D. H. McDaniel, Appl. Phys. Lett. **47**, 229 (1985).

[15] H. U. Rahman, P. Ney, F. J. Wessel, A. Fisher, and N. Rostoker, in *Dense Z-Pinches,* edited by N. Pereira, J. Davis, and N. Rostoker, AIP Conf. Proc. No. 195 (AIP, New York, 1989), p. 351.

[16] J. Delvaux, H. Lamain, C. Rouille, H. J. Doucet, J. M. Buzzi, M. Gazaix, and B. Etlicher, in *Proceedings of the Fourth International Topical Conference on High Power Electron and Ion Beam Research and Technology* (Ecole Polytechnique, Palaiseau, France, 1981), Vol. 2, p. 775.

[17] M. Gazaix, H. J. Doucet, B. Etlicher, J. P. Furtlehner, H. Lamain, and C. Rouille, J. Appl. Phys. **56**, 3209 (1984).

[18] Calculated using the Sandia National Laboratories' "X-Ray Detector" code, courtesy of R. B. Spielman.

[19] P. Audebert, H. Lamain, B. Dufour, C. Rouille, B. Etlicher, L. Voisin, and P. Romary, in *Proceedings of the Eighth International Conference on High Power Particle Beams* (World Scientific, Singapore, 1990), Vol. 1, p. 422.

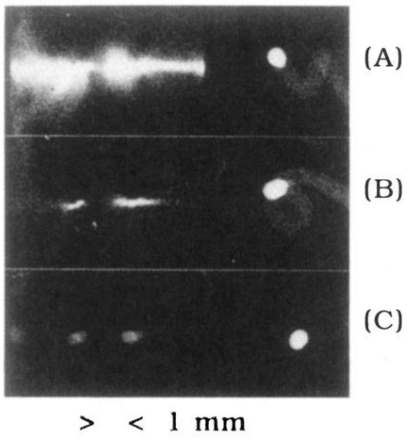

FIG. 2. Time-integrated x-ray pinhole images of an Al jet-only discharge: shot No. 1350, foil delay $\simeq$12.6 μs. Pinhole diameter/filter thickness: panel (A), 50-μm pinhole/25-μm Be; panel (B), 50-μm pinhole/1.5-μm Ta; panel (C), 200-μm pinhole/10-μm Ti filter.

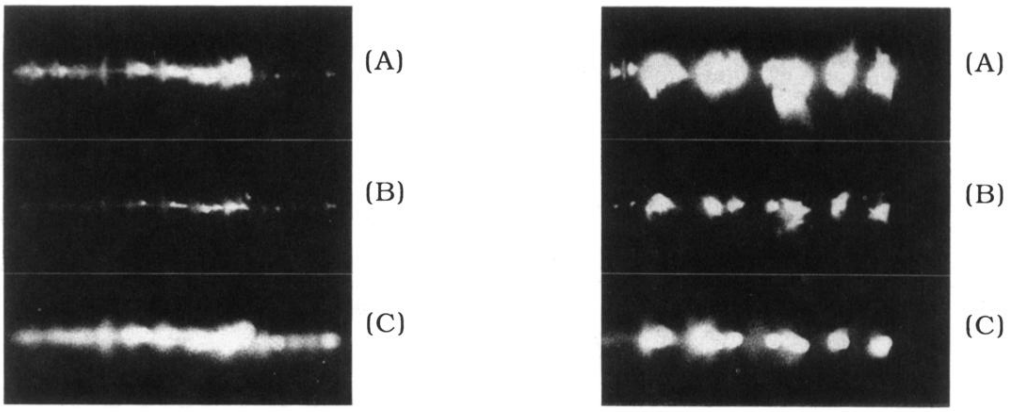

FIG. 3. X-ray pinhole images for two wire-only discharges: (a) shot No. 1379, 10-μm-diam W wire; (b) shot No. 1384, 20-μm-diam Cu wire. Same pinhole/filter combinations as Fig. 2.

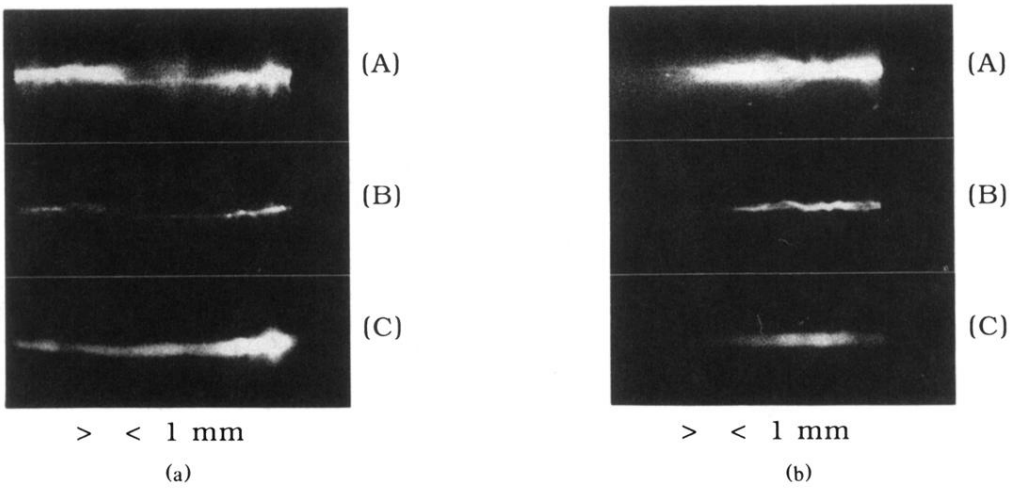

FIG. 4. X-ray pinhole images for two POW discharges: (a) shot No. 1378, 10-μm-diam W wire, foil delay 14.3 μs, and (b) shot No. 1386, 20-μm-diam Cu, foil delay 14.8 μs. Same pinhole/filter combinations as Fig. 2.

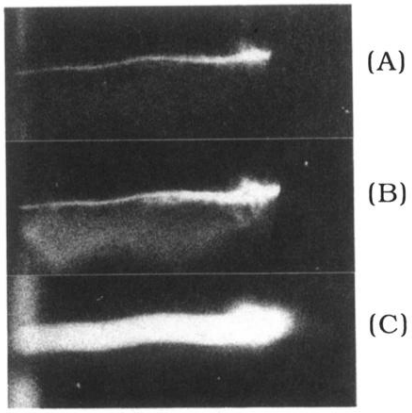

FIG. 5. X-ray pinhole images of a POW discharge with reduced liner mass: shot No. 1341, 10-μm-diam W, foil delay 7.6 μs. Pinhole diameter/filter thickness: panel (A), 50-μm pinhole/25-μm Be filter; panel (B), 50-μm pinhole/10-μm Be filter; panel (C), 400-μm pinhole/10-μm Ti filter.